Hydrol. Earth Syst. Sci., 12, 691–702, 2008
www.hydrol-earth-syst-sci.net/12/691/2008/

Hydrology and Earth System Sciences

Filter properties of seam material from paved urban soils

T. Nehls[1], **G. Jozefaciuk**[2], **Z. Sokolowska**[2], **M. Hajnos**[2], **and G. Wessolek**[1]

[1]Berlin Institute for Technology, Dept. for Ecology, Chair for Soil Conservation, Salzufer 11-12, 10587 Berlin, Germany
[2]Institute of Agrophysics of Polish Academy of Sciences, Doswiadczalna 4, 20-290 Lublin, Poland

Received: 9 August 2007 – Published in Hydrol. Earth Syst. Sci. Discuss.: 15 August 2007
Revised: 10 March 2008 – Accepted: 24 March 2008 – Published: 24 April 2008

Abstract. Depositions of all kinds of urban dirt and dust including anthropogenic organic substances like soot change the filter properties of the seam filling material of pervious pavements and lead to the formation of a new soil substrate called seam material.

In this study, the impact of the particular urban form of organic matter (OM) on the seam materials CEC_{pot}, the specific surface area (A_s), the surface charge density (SCD), the adsorption energies (E_a) and the adsorption of Cd and Pb were assessed. The Cd and Pb displacement through the pavement system has been simulated in order to assess the risk of soil and groundwater contamination from infiltration of rainwater in paved urban soils.

A_s, E_a and SCD derived from water vapor adsorption isotherms, CEC_{pot}, Pb and Cd adsorption isotherms where analyzed from adsorption experiments. The seam material is characterized by a darker munsell-color and a higher C_{org} (12 to 48 g kg^{-1}) compared to the original seam filling. Although, the increased C_{org} leads to higher A_s (16 m^2 g^{-1}) and higher CEC_{pot}(0.7 to 4.8 cmol$_c$ kg^{-1}), with 78 cmol$_c$ kg^{-1}C its specific CEC_{pot} is low compared to OM of non-urban soils. This can be explained by a low SCD of 1.2×10^{-6} mol$_c$ m^{-2} and a low fraction of high adsorption energy sites which is likely caused by the non-polar character of the accumulated urban OM in the seam material.

The seam material shows stronger sorption of Pb and Cd compared to the original construction sand. The retardation capacity of seam material for Pb is similar, for Cd it is much smaller compared to natural sandy soils with similar C_{org} concentrations. The simulated long term displacement scenarios for a street in Berlin do not indicate an acute contamination risk for Pb. For Cd the infiltration from puddles can lead to a breakthrough of Cd through the pavement system during only one decade. Although they contain contaminations itself, the accumulated forms of urban OM lead to improved filter properties of the seam material and may retard contaminations more effectively than the originally used construction sand.

Correspondence to: T. Nehls
(thomas.nehls@tu-berlin.de)

1 Introduction

In urban areas, sealing of soil surfaces leads to ecological problems caused by the increased and accelerated runoff and reduced evapotranspiration compared to non-sealed soils. Cities are normally drier and hotter than the surrounding areas. At heavy rainfalls the exceeding water causes mixed sewage systems to run over. This is one of the main threats to water quality of urban water bodies (Heinzmann, 1998). Therefore, run off reduction by increasing infiltration is among the main ideas of ecological urban planning. This goal can be reached by increased use of pervious pavements. In many European cities, especially in the older parts, they are regularly found. They keep the convenience for the city dwellers but allow infiltration rates of 58 cm d^{-1} for a mosaic tile pavement with 20 % of seams, until 155 cm d^{-1} for so called grass pavers having a coverage of open seams of up to 41% (Wessolek and Facklam, 1997).

The seams allow infiltration and the pavers reduce evaporation. Therefore, groundwater recharge rates are 99 to 208 mm a^{-1} in sealed areas compared to only 80 mm a^{-1} for a pine-oak forest around Berlin (Wessolek and Renger, 1998). If rain water accumulates in puddles on the pavements, the groundwater recharge can be greater than 300 mm a^{-1}. Puddles with up to 60 mm depth are no exception in old quarters. We gauged a puddle in front of our department (52°31′4.03′ N; 13°19′25.79′ E) with a volume of 56 L at a horizontal projection of only 2 m^2. Rainwater runoff in urban areas is often contaminated, e.g. by heavy metals. Dannecker et al. (1990) and Boller (1997) found Pb

Fig. 1. Dark seam material (0 to 1 cm) compared to the lighter original sandy seam filling (1 to 5 cm) at the sidewalk at Pfluegerstrasse, Berlin.

concentrations of up to 0.3 mg L^{-1} in the street runoff, while *Cd* concentrations reached up to 0.0076 mg L^{-1} (Dierkes and Geiger, 1999). The high infiltration rates might result in high contaminant fluxes even if dissolved contaminant concentrations are low (Dannecker et al., 1990). An assessment of the risk of soil and groundwater contamination requires hydraulic and sorption parameters for the pavers and the construction material, mainly sand. Furthermore, after a while, a new horizon, the "seam material", develops. The term "seam material" describes the soil material in between single pavestones of pavements, which developed from technogenic sand. It has a black or brownish black color according to Munsell soil color table, is mostly only 1 cm thick and contains all kinds of deposited urban dirt like foliage, hairs, oil, dog faeces, food residues, cigarette stubs, glas – in short: any kind of urban waste, small enough to fit into the pavement seams, at least after being milled by pedestrians or cars. Thereby, pedestrians and cars abrase their soles and tires and these abrasions also end up in the seams. Furthermore seams contain great portions of urban dust and therefore soot, concrete abrasions, aerosols and so on. While the hydraulical characteristics of the seam material have already been investigated (Nehls et al., 2006), the chemical filter properties are still unknown. They can not be extrapolated from other soils because the organic carbon (C_{org}) of this material differs from non-urban, natural soils in origin, quality and function. For instance, the percentage of black carbon, a "combustion-produced black particulate carbon, having a graphitic microstructure" (Novakov, 1984) on C_{org} is increased compared to non-urban soils (own unpublished data). It is hypothesized, that because of its increased C_{org} contents, seam material acts as a valuable filter and influences transport processes through the pavement seams. Therefore, the motivation of this study was to assess the seam materials retardation potential for heavy metals under consideration of its special forms of organic matter, its source or sink function and its thickness. Therefore, (i) general surface and filter properties of the seam material were investigated in relation to C_{org} by ion exchange and water vapor adsorption measurements. Cation exchange capacity, surface area, surface charge density, and adsorption energy were studied. Thereby, the OM itself could be characterized. Furthermore, (ii) the seam materials specific adsorption of Pb and Cd, two relevant toxic heavy metals of different mobility and affinity to organic matter, were exemplarily studied. Finally, (iii) the heavy metal solute transport through the pavement system considering the seam material have been simulated using the investigated parameters.

2 Material and methods

2.1 Sites and sampling

Samples were taken in Berlin and Warsaw, two cities with similar climatic, geologic and geomorphologic conditions, but different industrial activity, traffic intensity and contamination history. The sampling sites were located close to roads or directly on roads.

Samples consisted of the material that fills spaces between single stones of pavements. The dark seam material at 0 to 1 cm depth was always easily distinguishable from a much brighter 1 to 5 cm layer (Fig. 1). The upper layer is influenced by all external factors and deposits, while the deeper one was taken as representative of the original seem filling material, which is not severely altered by external deposits. The seam material was scraped up using one–way polyethylene teaspoons - once, under suspicious observation of the police.

In Berlin (B-samples), we sampled both the seam material and the original seam filling layer, while only the upper layer was sampled in Warsaw (W-samples). Samples were taken in the following streets: Monbijouplatz (B1, B1a), Weidendamm (B2, B2a), Schnellerstrasse (B3, B3a), from different places at the Grosser Stern (B4–B8, B4a), Emilii Plater (W1), Jerozolimskie (W2), Pulawska (W3), Rzymowskiego (W4), Stanow Zjednoczonych (W5), Modlinska (W6), Slowackiego (W7), Wilanowska (W8) and Rowecki Bridge (W9). Sampling sites were located on sidewalks within 2 m from roads with different traffic intensity, while samples from the Pfluegerstrasse (B9, B10) were sampled directly on the road. Samples B1a-B4a have been taken from the same sites as B1 to B4, the index "a" indicates that samples consist of original seam filling material (1 to 5 cm).

2.2 General chemical properties

Munsells's color was determined for fresh samples. The pH($CaCl_2$) and electric conductance (EC) have been

measured using standard methods (DIN-ISO 10390, DIN-ISO 11265).

The samples W8 and W9 showed higher EC than the other samples (see Table 2). Together with the Berlin samples B2 and B9 they have been additionally analysed for Cl^- and SO_4^{2-} using capillary electrophoresis (Agilent 3D CE). It has been calculated how much of the measured EC is caused by Cl^- and SO_4^{2-} following the empirical relation between EC [mS cm^{-1}] and ionic strength I [mol L^{-1}] at 298 K given by Griffin and Jurinak (1973):

$$I \cong 0.013\, EC \tag{1}$$

and the relationship between individual ion concentration c_i [mol L^{-1}], its valency z_i [-] and I:

$$I = 0.5 \sum c_i z_i^2 \tag{2}$$

The potential cation exchange capacity (CEC_{pot}) was determined at pH 8.2 using a batch method with cation exchange and re-exchange (Mehlich, 1984) because of high EC of the samples. The total carbon content, C_{tot} and C_{org} were determined conductometrically after combustion (Carlo Erba, C/N analyzer, C_{org} after HCl-treatment to remove carbonates).

2.3 Surface properties

The specific surface area (A_s) and the adsorption energies (E_a) were calculated from water vapor adsorption isotherms using the vacuum chamber method at the temperature T=294±0.1 K. Prior to the adsorption measurement, soil sample aliquots of 3 g were dried in a hermetic chamber with concentrated sulphuric acid until constancy of weights. Then, they were exposed to 20 stepwise rising water vapor pressures (p/p_s) ranging from 0.005 to 0.98 which were controlled by sulfuric acid solutions. The samples were equilibrated with the corresponding water vapour until constancy of weights. The higher p/p_s is, the longer the time gets for equilibration, at the highest step more then one week was necessary. The mass of adsorbed water, a, was the difference between the weight of the humid sample and the dry sample (dried for 24 h at 378 K). Results of triple weightings had a coefficient of variation (CV) of 3.7 %, averaged values were used for further calculations.

Aranovich's theory of polymolecular adsorption has been used to obtain the capacity of a mono-molecular layer from the experimental water vapour adsorption isotherms (Fig. 2). In contrast to the standard Brunauer-Emmett-Teller (BET) model (Brunauer et al., 1938), Aranovich's isotherm allows vacancies in the adsorbed layer and describes the polymolecular adsorption over a broader and more realistic range of p/p_s ($\approx 0.05 < p/p_s < 0.8$) than the BET does ($\approx 0.05 < p/p_s < 0.3$) (Aranovich, 1992):

$$a = \frac{a_m\, C\, p/p_s}{(1 + C\, p/p_s)\, \sqrt{(1 - p/p_s)}}, \tag{3}$$

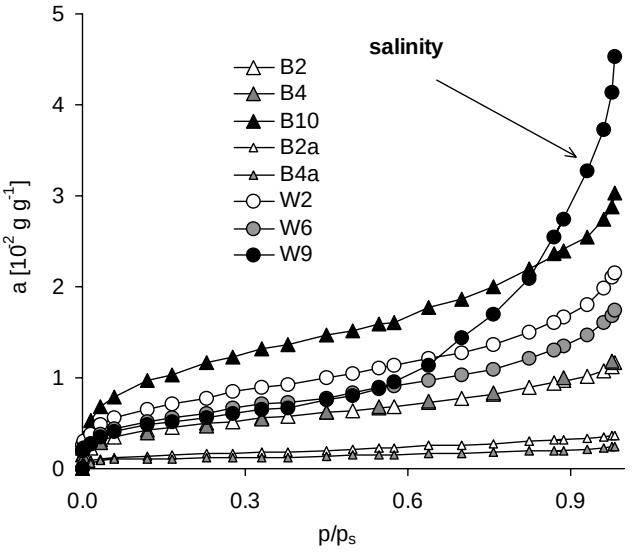

Fig. 2. Measured water-vapor adsorption isotherms for seam material of pavements in Berlin (B) and Warsaw (W); (a=mass of adsorbed water, p/p_s=water vapour pressure).

where p/p_s [Pa Pa^{-1}] is the water vapour pressure , a [g] is the adsorbed water at a given p/p_s, a_m [g] is the statistical monolayer capacity and $C = e^{\frac{\bar{E}_a - E_c}{RT}}$, a constant related to the adsorption energy, $\bar{E}_a$ [J] and condensation energy of water, E_c [J].

Aranovich's isotherm was fitted to the experimental data (measured a vs. adjusted p/p_s) to derive values for a_m and C.

Having a_m, we calculated A_s [m^2] of the sample using the following equation:

$$A_s = \frac{a_m\, L\, \omega}{M}. \tag{4}$$

Here, L is the Avogadro number (6.02×10^{23} molecules per mole), M [g mol^{-1}] is the molecular mass of the adsorbate and ω is the area occupied by a single adsorbate molecule (1.08×10^{-19} m^2 for water). Knowing A_s, the surface charge density SCD [cmol$_c$ m^{-2}] can be calculated:

$$SCD = \frac{CEC_{pot}}{A_s}, \tag{5}$$

The adsorption energy distribution functions showing fractions f of surface sites of different adsorption energies, ($f(E_i)$), were calculated from adsorption isotherms data, using the theory of adsorption on heterogeneous surfaces (Jaroniec and Brauer, 1986). Aranovich's isotherm (Aranovich, 1992) was applied to describe local adsorption effects in the total adsorption isotherm Θ_T(p), which is the sum of

Table 1. Input parameters for the numerical simulation of heavy metal displacement through a pavement soil column. Θ_r residual water content, Θ_s water content at saturation, α 1/matric potential at air entry, n fitting parameter, K_S water conductivity at saturation, ρ_B dry bulk density, $K^*_{S1,2}$ and Θ^*_s indicate derived effective model parameters for realizing the two chosen water flow conditions, $K_f(Pb, Cd)$ Freundlich's equilibrium constant for Pb and Cd, m Freundlich's exponent for Pb and Cd, $c_{Pb,Cd}$ dissolved heavy metal concentrations.

general model parameters								
length unit: cm, time unit: d, mass unit: mg length of the column: 20 cm; number of nodes: 101 upper boundary condition: constant pressure head Ψ_u lower boundary condition: constant pressure head Ψ_l								
	seam material				construction sand			
soil hydraulic parameters								
Θ_r $\left[\mathrm{cm^3\,cm^{-3}}\right]$	0.117				0.058			
Θ_s $\left[\mathrm{cm^3\,cm^{-3}}\right]$	0.527				0.424			
α $\left[\mathrm{cm^{-1}}\right]$	0.034				0.058			
n $[-]$	1.514				1.401			
K_S $\left[\mathrm{cm\,d^{-1}}\right]$	715				374			
ρ_B $\left[\mathrm{g\,cm^{-3}}\right]$	1.16				1.51			
water flow parameters in the model								
$\Psi_u = \Psi_l$ [cm]	0							
$K^*_{S1,2}$ $\left[\mathrm{cm\,d^{-1}}\right]$	0.12, 0.48							
Θ^*_s $\left[\mathrm{cm^3\,cm^{-3}}\right]$	0.264 for K^*_{S1} (0.298 for K^*_{S2})				0.231 for K^*_{S1}(0.265 for K^*_{S2})			
adsorption parameters								
	B1	B2	B4	B9	B1a	B2a	B4a	B9a
K_f(Pb) $\left[\mathrm{mg^{1-m}\,L^m\,kg^{-1}}\right]$	2638	2133	1321	1416	499	272	833	738
m(Pb) $[-]$	1.00	1.00	0.45	0.62	0.92	1.00	0.55	0.62
c_{Pb}(soil water)$\left[\mathrm{mg\,L^{-1}}\right]$	0	0.22	0.02	0.04	0.04	0.46	0.01	0.01
c_{Pb}(rainwater)$\left[\mathrm{mg\,L^{-1}}\right]$	0.3							
$K_f(Cd)[\mathrm{mg^{1-m}\,L^m\,kg^{-1}}]$	20.38	16.95	19.37	15.18	6.92	5.41	5.66	8.61
m(Cd) $[-]$	0.70	0.38	0.62	0.28	0.63	0.41	0.40	0.34
c_{Cd}(soil water)$\left[\mathrm{mg\,L^{-1}}\right]$	0.013	0.020	0.004	0.020	0.023	0.013	0.020	0.019
c_{Cd}(rainwater)$\left[\mathrm{mg\,L^{-1}}\right]$	0.01							

adsorptions on sites of energy E_i, weighted by their fractions, $f(E_i)$:

$$\Theta_T(p) = \frac{1}{\sqrt{1-x}} \sum_{i=1}^{n} \frac{C_i\, x}{(1 - C_i\, x)\, f(E_i)}. \quad (6)$$

Here, x = p/p_s and C_i is the value of the constant C for sites of kind i. Solving Eq. (6) for $f(E_i)$ is an ill-conditioned problem. Small variation in experimental data caused by heterogeneity of the samples and detections capabilities of the balance leads to large variation in estimation of site fractions. Therefore, a condensation approximation CA was inserted (Harris, 1968). This method is based on the replacement of the local isotherm by a step-function. The final formula for the calculation of site fractions then becomes:

$$f(E_i) = \frac{\sqrt{1-x_{i+1}}\;\Theta_\tau(E_{i+1}) - \sqrt{1-x_i}\;\Theta_\tau(E_i)}{E_{i+1} - E_i}. \quad (7)$$

From $f(E_i)$ values, the average water vapor adsorption energy, $\bar{E}_a$, can be calculated by the following equation as described by Jozefaciuk and Shin (1996):

$$\bar{E_a} = \sum E_i\; f(E_i). \quad (8)$$

Table 2. Surface properties and general characteristics of seam materials and original seam fillings from Berlin and Warsaw. Values in one column followed by the same letter are not significantly different at $p<0.05$; N=20.

Site	Munsell Color	pH ($CaCl_2$)	EC $\mu S\,cm^{-1}$	CEC_{pot} $cmol_c\,kg^{-1}$	C_{tot} $g\,kg^{-1}$	C_{org} $g\,kg^{-1}$	$A_s(H_2O)$ $m^2\,g^{-1}$	SCD $\mu mol_c\,m^{-2}$	$\bar{E}_a$ J
Berlin, 0 to 1 cm									
B1	2.5Y3/2	6.8	107 b	1.8	19.2	14.3	14.8	1.2	3.1
B2	2.5Y3/2	7.1	93 b	1.6	18.7	16.2	12.4	1.3	3.2
B3	2.5Y2.5/1	7.1	–	2.0	33.4	27.6	17.0	1.2	2.8
B4	2.5Y3/1	7.2	143 b	2.0	25.5	23.2	12.2	1.6	3.3
B5	2.5Y3/1	7.3	161 b	1.9	23.0	21.8	13.6	1.4	3.1
B6	2.5Y3/1	6.8	76 b	1.2	17.6	12.0	8.9	1.4	3.4
B7	2.5Y3/1	7.2	87 b	1.2	21.0	18.6	12.7	1.0	3.1
B8	2.5Y3/1	7.1	101 b	1.3	15.8	13.1	11.0	1.2	3.2
B9	10YR2/1	7.1	79 b	1.8	22.9	18.4	14.0	1.3	3.0
B10	10YR2/1	6.6	114 b	4.8	52.7	48.2	29.3	1.6	2.8
Berlin, 1 to 5 cm									
B1a	10YR4/6	7.1	48 c	0.8	5.1	3.8	7.5	1.0	3.4
B2a	10YR5/6	7.0	21 c	0.2	1.8	1.7	5.3	0.3	3.9
B3a	2.5Y4/3	7.1	–	–	4.4	3.1	5.2	n.d.	3.9
B4a	2.5Y5/3	7.1	28 c	0.4	2.2	0.2	3.0	1.4	4.3
Warsaw, 0 to 1 cm									
W1	2.5Y2.5/1	–	306 a	2.1	29.5	22.8	13.8	1.5	–
W2	2.5Y2.5/1	6.9	402 a	1.9	43.4	35.4	20.4	0.9	3.1
W3	2.5Y2.5/1	7.4	328 a	3.4	32.3	27.9	27.8	1.2	2.9
W4	2.5Y3/1	7.4	409 a	1.7	26.9	20.8	12.8	1.3	2.8
W5	10YR2/1	7.3	426 a	2.1	35.6	27.9	17.8	1.2	2.7
W6	2.5Y3/1	7.3	440 a	1.5	32.3	25.7	15.8	0.9	2.9
W8	2.5Y3/1	7.2	2040 a	0.7	18.7	12.4	11.3	0.6	2.6
W9	2.5Y3/2	7.4	1927 a	1.2	21.8	15.6	14.9	0.80	1.3

The calculation of adsorption energy distribution functions ($f(E_i)$ vs E_i) was performed using Eq. (7). Energy values were expressed in the units of thermal energy (RT), as scaled energies ($\frac{\bar{E}_a - E_c}{RT}$). A scaled energy equal to 0 represents an adsorption energy equal to the condensation energy of the vapor. The maximum adsorption energy in the condensation approximation is related to the minimum value of p/p_s which was around 0.004 in our case. This corresponds to an energy adsorption of around –5.5. Thus, it was reasonable to assume –6 as the maximum energy for the samples. However, this value can be considered only as a first estimate of the maximum energy because of the lack of experimental data at small relative pressures. We arbitrarily set the maximum energy to –8 assuming that if there were no sites with higher adsorption energies than –6, the corresponding values of $f(E_i)$ will be close or equal to zero. In order to reduce the noise of the measurements, only pairs of values of $f(E_i)$, which differ for at least 2 units were used.

2.4 Adsorption isotherms for Cd and Pb

Adsorption isotherms were obtained for C_{org} affected, immobile Pb and mobile Cd according to OECD guideline 106 (OECD, 2000). One gram of soil has been equilibrated with 45 ml 0.01 M $CaCl_2$ overnight. Then, Pb and Cd were added in 5 ml 0.01 M $CaCl_2$ solution for 48 h of equilibration. For all samples five stepwise rising solute concentrations beginning with destilled water were added. Therefore, the resulting adsorption isothermes include one desorption step and span over a wide range of concentrations (dissolved concentrations range from 0.05 to 10 mg L^{-1} for Pb and from 0.001 to 5 mg L^{-1} for Cd). After two hours of shaking, the original pH of the samples were re-adjusted with KOH. Dissolved phase HM concentrations were measured in the supernatant after 20 min of centrifugation at $1000\times g$.

The corresponding solid phase concentration was analyzed like following. In order to consider only the HM fraction which is involved in adsorption processes, the 0.025 M $(NH_4)_2$EDTA (pH 4.6) extractable portion has been determined (Welp and Brümmer, 1999) in advance for the

Fig. 3. Undisturbed sampling of seam material (0 to 1 cm) from a cobbled stone paved street using special 3.3 cm^3 cylinders in an old residential area at the site Pfluegerstrasse, Berlin.

individual samples. The samples were extracted with concentrated HNO_3 (soil/acid ratio=1/20) for 360 min at 453 K under pressure. The difference of HNO_3 and EDTA extract is the residual concentration which has not been considered as adsorbed phase.

For the fitting of an adsorption isotherm to the experimental data with complex solid phases like soils, the use of the Freundlich model is widely recommended (Stumm and Morgan, 1996):

$$C_s = K_f \, C_l{}^m \quad , \tag{9}$$

where C_s [mg kg^{-1}] is the sorbed concentration in the solid phase, C_l [mg L^{-1}] is the dissolved concentration, K_f [mg^{1-m} L^m kg^{-1}] is the Freundlich distribution coefficient, describing the soil material's affinity to the solute. The exponent m is a measure for the linearity of the adsorption.

Freundlich's model is favoured before Langmuir, because it does not expect similar energy sites but can be seen as a sum function of Langmuir isotherms for the individual energy sites (Sposito, 1980). So it is adequate to describe the seam material which is a mixture of sorbents with varying surface characteristics and adsorption energy sites.

The adsorption characteristics are studied to describe the mobility of the heavy metals. A good method to compare different adsorption characteristics with different degrees of linearity is to calculate the retardation factor R, which derives from the convection-dispersion equation and describes the retardation of substances compared to a conservative, non sorbing tracer:

$$R = 1 + \frac{\rho_B}{\Theta} \frac{\partial C_s}{\partial C_l} \quad , \tag{10}$$

where ρ_B [g cm^{-3}] is the dry bulk density and Θ [m^3 m^{-3}] is the water content of the soil. For non-linear adsorption of solutes described by Freundlich's model R becomes:

$$R = 1 + \frac{\rho_B}{\Theta} m K_f C_l^{m-1} \quad . \tag{11}$$

2.5 Simulation of the Cd and Pb displacement

The filter effect of the seam material has been assessed by a numerical HM displacement simulation using the software HYDRUS 1D v2.02 (US Salinity Laboratory USDA-ARS, 1991, Riverside, CA, USA). It solves the Richards equation numerically and applies the convection dispersion equation for the solute transport. It also includes Freundlich's adsorption model (Simunek et al., 1999). The employed input data are shown in Table 1.

It was the goal to assess the impact of the chemical properties (special form of OM), the importance (thickness) and the source/sink function (contamination status) of the seam material on heavy metal displacement. The travel times were simulated through a 20 cm long column of (i) construction sand, (ii) a 1 cm thick seam material and 19 cm of construction sand and (iii) 20 cm of seam material. The soil hydraulical parameters of the site B9 have been applied while the chemical features of the sites B1, B2, B4 and B9 have been used for the simulation. Travel time in that context indicates the period of time which is required to recover 95 % of the upper boundary concentration at the lower boundary of the column. The measured background concentrations in the soil were (*a*) ignored (no contamination) and (*b*) considered as initial conditions. So, six scenarios *ia, ib, iia, iib, iiia, iiib* have been simulated. Scenarios *ia* and *iiia* compare the maximum retardation capacity of the original construction material with that of the seam material, while in *iia* the maximum retardation of the realistic soil material mixture is assessed. The scenarios *a* and *b* are then used to assess the actual source/sink potential of the construction sand and the seam material.

Groundwater recharge rates of 120 mm a^{-1} and of 480 mm a^{-1} (simulating infiltration from puddles) were applied (Wessolek and Renger, 1998). Furthermore, the open seam surface area of 27 %, measured at site B9, was included to get the daily groundwater recharge rates of 0.12 and 0.48 cm d^{-1} for the open seam area as the net infiltration rate at the upper boundary. Thus, annual evapotranspiration has been indirectly considered, but seasonal variations have been disregarded. The water flow was not simulated but realized by accordingly chosen boundary conditions and derived effective parameters for the site B9: K_s^* of 0.12 and 0.48 cm d^{-1}, respectively and pressure heads of 0 cm for the upper and lower boundary conditions. The according artificial saturated water contents, Θ_s^* corresponded to K_s^* and were derived from $K(\Psi)$ and $\Theta(\Psi)$ functions fitted to measured porosity (Nehls et al., 2006) and K_s data (Table 1). For K_s measurements, 100 cm^3 cylinders were filled with seam

material up to bulk densities which have been determined using small cylinders which fitted in the intersection of seams on the cobble stone paved street at site B9 (Fig. 3 and Nehls et al., 2006). For the original construction sand, undisturbed cylinders were taken from the layer beneath the pavestones.

For simulating the actual HM contaminations of the materials, their dissolved equilibrium concentrations were measured and applied (see Table 1).

The infiltrating water can be contaminated too. Rain water runs over the pavements takes up soluble contaminants and accumulates in puddles and infiltrates and evaporates or infiltrates directly through the seams. The concentrations of this infiltrating surface water at the upper boundary for Pb and Cd were chosen to be 0.3 and 0.01 mg L^{-1}, respectively.

3 Results and discussion

3.1 General and surface properties

The seam material shows a neutral soil reaction with an average pH of 7.1 (SD=0.2, N=17), which is typical for urban soils. It is most likely caused by concrete abrasions from buildings (Burghardt, 1994). For the seam material, additionally the adjacent pavers can be direct sources of constant carbonate supply as pedestrians not only abrase the soles of their shoes but also the surface of concrete or limestone pavers. The difference of C_{tot} and C_{org}, most probably carbonates, is 5 g kg^{-1} (SD=2 g kg^{-1}, N=18).

The EC is significantly higher in Warsaw compared to Berlin ($p<0.05$, N=20) (Table 2). The reason for that is most probably a more frequently use of deicing salts on streets of Warsaw compared to Berlin (see below). There was no difference between the seam material and the original construction sand detectable.

The seam material is dark. The Munsell colors objectively prove and quantify this observation (Table 2). Like in "natural" soils this coloration can be explained by an enrichment of OM, which in this case could be black soot. Measured C_{org} varies from 12 to 48 g kg^{-1} in the 0 to 1 cm layer and is higher than in the 1 to 5 cm layer (less than 3 g kg^{-1}) (Table 2). A displacement of C_{org} into the 1 to 5 cm layer can be expected (Fig. 1). However, the low C_{org} contents in the 1 to 5 cm layers allow to regard it as original and only slightly altered. Besides that, it cannot be excluded, that the construction sand already contained different concentrations and forms of OM.

The CEC_{pot} of the 0 to 1 cm layer in Berlin is not significantly different from that in Warsaw. With 1.2 to 4.8 $cmol_c$ kg^{-1} the CEC_{pot} of the seam material is low compared to values of 12 to 20 $cmol_c$ kg^{-1} for non-urban German sandy soils (Renger, 1965) or compared to values of 8 to 36 $cmol_c$ kg^{-1} for Berlin sandy forest soils with similar C_{org} contents (Wilczynski et al., 1993).

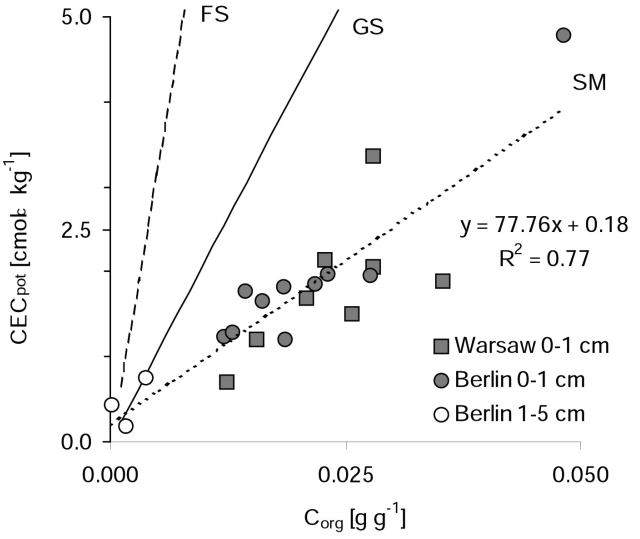

Fig. 4. Relationship between organic carbon content (C_{org}) and potential cation exchange capacity (CEC_{pot}) in seam materials (SM, doted), sandy German soils (GS, solid) (Renger, 1965) and sandy forest soils (FS, dashed) (Wilczynski et al., 1993).

With 0.5 $cmol_c$ kg^{-1} soil, the CEC_{pot} of the 1 to 5 cm layer is significantly smaller than in the first layer. Compared to the original seam filling represented by the 1 to 5 cm layer, the depositions of urban dirt lead to an approximately four times higher CEC_{pot} in the seam material. Like for other sandy soils the CEC_{pot} of the seam material depends mainly on OM (Renger, 1965). The CEC_{pot} of seam materials is proportional to A_s which depends on C_{org} (Figs. 4 and 5). Both regression lines intersect the y-axis close to (0;0), which indicates that only C_{org} compounds contribute substantially to A_s and to CEC_{pot}.

Due to it's special quality, the contribution of the seam material's C_{org} to CEC_{pot} is only 78 $cmol_c$ kg^{-1}C, (Fig. 4). However, the CEC_{pot} of non-urban soil OM has been estimated to be around 300 $cmol_c$ kg^{-1}C by Parfitt et al. (1995) for New Zealand soils and by Krogh et al. (2000) for Danish soils. Higher CEC_{pot} of up to 680 $cmol_c$ kg^{-1}C were observed in acidic sandy forest soils (Wilczynski et al., 1993).

As mentioned above, the OM of seam materials consist of different constituents, not everything can be referred to as humus. Black carbon (BC) for instance accounts for up to one third of the C_{org} fraction (own unpublished data). Although BC contributes to the CEC_{pot} of soils, its contribution is lower than that of humus (Tryon, 1948).

Assumed, the CEC_{pot} of the seam material is solely depending on C_{org} (axis intersection at CEC_{pot}=0), the CEC_{pot} of the OM rises, if not $C=C_{org}$, but $C=C_{org}-BC$ is applied for the correlation (85 $cmol_c$ kg^{-1}C, r^2=0.77 for C_{org} and 97 $cmol_c$ kg^{-1}C, r^2=0.77 if $C=C_{org}-BC$ is applied).

The low contribution of seam materials C_{org} to CEC_{pot} can be explained by its low specific surface area (Fig. 5) and its low surface charge density. The first of the two reasons can

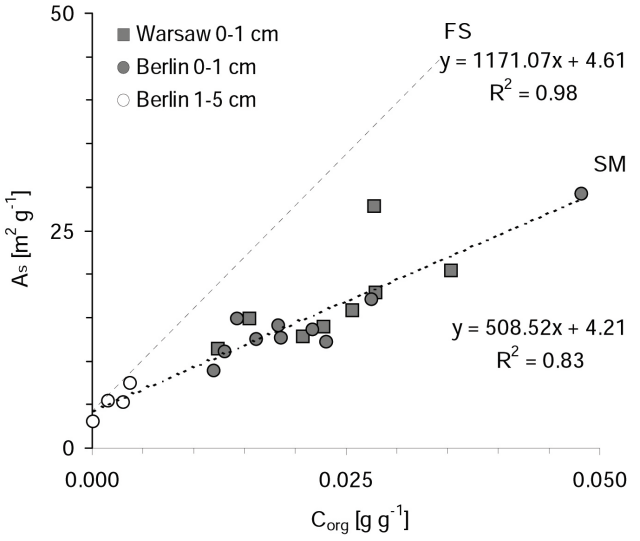

Fig. 5. Contribution of seam material's C_{org} (SM) to specific surface area measured by water vapour desorption isothermes A_s compared to forest soil's C_{org} (FS) investigated by Wilczynski et al. (1993).

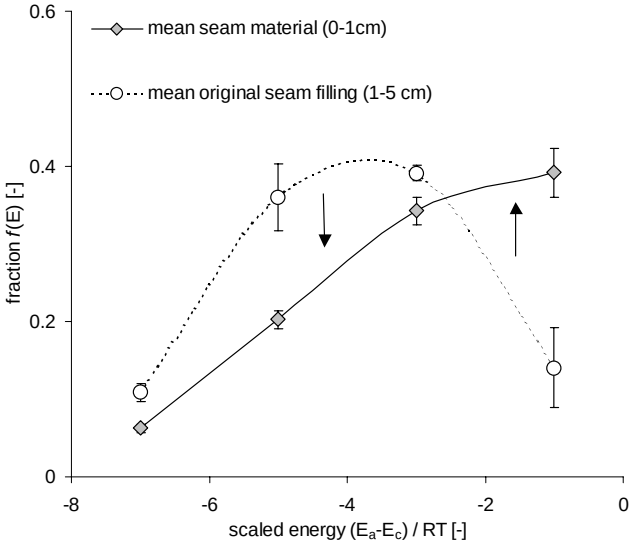

Fig. 6. Distribution of scaled adsorption energy levels for seam materials and original seam filling (sand) from Berlin and Warsaw. The arrows indicate the shift in adsorption energy fractions due to the deposition of urban dust. Error bars show standard errors, N = 19 for seam materials, N=4 for original seam filling.

be ascribed to the spheroidal particulate character of the C_{org} (Nehls et al., 2006) resulting in low A_s (presuming similar substance densities) compared to humus. The samples from Berlin and Warsaw show a similar behavior resulting in a strong correlation between C_{org} and A_s (r^2=0.8). As it can be seen from the slope of the linear regression line, A_s of the seam material's C_{org} is about $509\,m^2\,g^{-1}C$. Wilczynski et al. (1993) investigated a Berlin forest soil using the same methodology for measuring A_s and found the contribution of C_{org} to A_s to be up to $1062\,m^2\,g^{-1}C$.

The SCD of a soil sample is a measure for the quantity of polar functional groups. The SCD of the seam material is seven times lower than that of sandy forest soils (Wilczynski et al., 1993; Hajnos et al., 2003), which causes the comparable low CEC at similar C_{org} levels (Fig. 4). Hajnos et al. (2003) report a SCD of 2.9 to $10.6\times10^{-6}\,mol_c\,m^{-2}$ for Berlin sandy forest soils, while the SCD of seam material is not greater than $1.2\times10^{-6}\,mol_c\,m^{-2}$. The low SCD of the seam material's C_{org} likely is caused by unpolar organic substances.

This statement is supported by the distribution of E_a (Fig. 6). Medium energy sites dominate in the original construction sand. In the studied seam materials the water binding forces are lower. Most of the seam materials show a high number of low energy sites and only a low number of higher energy sites. This indicates a higher fraction of polar surfaces in the lower layer. The shift between the construction sand and the seam material is caused by the accumulation of non-polar substances, mainly OM. Additionally, the organic substances may have coated polar mineral surfaces in the upper layer.

Higher polarity (indicated by $\bar{E}_a$) usually results in higher SCD. However, there is no dependence between $\bar{E}_a$ and SCD for the seam material. Likely, the low $\bar{E}_a$ is caused by the adsorption of water by deicing salts, which are mainly NaCl, sometimes $CaCl_2$ and $MgCl_2$, and $CaSO_4$ as impurity. For samples W8 and W9, Cl^- is 0.349 and $0.413\,g\,L^{-1}$, SO_4^{2-} is 0.019 and $0.045\ g\,L^{-1}$ respectively. Cl^- alone causes 37 and 46 % of the EC of samples W8 and W9, Cl^-together with SO_4^{2-} causes 40 and 53 % of the measured EC (see Table 2). The latter percentage is likely caused by calculation of EC from I by the equation of Griffin and Jurinak (1973) which was derived empirical for natural aquatic systems and soil extracts not including pavement seam materials. Different accuracies of the EC measurements compared to the electrophoresis measurements may also play a role. In samples B2 and B9 Cl^- is 0.0003 and $0.0014\,g\,L^{-1}$ and causes only 0.6 and 4 % of the measured EC. Different to the Warsaw samples the influence of SO_4^{2-} for B2 and B9 with concentrations of 0.002 and $0.004\,g\,L^{-1}$ is higher. Cl^-together with SO_4^{2-} causes 9 and 21 % of the measured EC for B2 and B9. This indicates, that for B2 and B9 deicing salts play not the same important role as for W8 and W9.

We found $\bar{E}_a$ decreasing with increasing EC which is related logarithmically with low hydration energy of the salt cations. Similar relations of adsorption energy and soil salinity parameters are observed in natural saline environments (Jozefaciuk et al., 1996; Toth and Jozefaciuk, 2002).

3.2 Heavy metal adsorption

The Freundlich K_f values for Pb and Cd are higher in the 0 to 1 cm layer than in the 1 to 5 cm layer. The values for m are similar for both depths. However, a comparison of K_f without considering m is not meaningful. Therefore, the retardation factors were calculated, which consider both parameters. They vary from 2056 to 94817 for Pb and from 42 to 485 for Cd for chosen ρ_B=1.5 g cm^{-3}, c_l=0.1 mg L^{-1}, Θ=0.3 m^3 m^{-3} (Table 3). Thereby, the seam material retards Pb stronger than the original construction sand.

3.2.1 Pb adsorption

For samples from Berlin, the higher adsorption potential of the seam material compared to the construction sand corresponds to higher C_{org} contents, which is expressed by the correlation of the retardation factor, R and C_{org} [g g^{-1}] (R=281986 C_{org} + 3600; r^2=0.82). Thereby, two samples have been excluded from the dataset: B1 and B2. For both samples, the Freundlich parameters were fitted with a specified range for m: 0≤m≤1 to meet the conditions for Freundlich's model stated by Sposito (1980).

There is no correlation of C_{org} and R for the Warsaw samples. The samples from Warsaw have higher R (p<0.05, N=9) at similar C_{org}, caused by higher K_f (p<0.05, N=9) and similar values for m. Following Sposito (1980) that indicates a higher variance of adsorbers in Warsaw, providing adsorption sites with a broader range of Pb adsorption energies. This might be due to, (i) a different kind of OM in Warsaw, which provides more adsorption sites for Pb compared to Berlin. However, this is not supported by different water adsorption energies (E_a) nor by different surface areas or different EDTA-extractable and total Pb concentrations.

More likely, it shows (ii) the greater importance of other adsorbers than the studied organic substances for the Warsaw samples. In Berlin, Pb_{tot} correlates closely with C_{org}, indicating same sources, e.g. combustion processes and/or strong adsorption of Pb on OM. However, the lacking correlation for the Warsaw samples could also be an effect of (iii) the small number of samples compared to the high spatial variability in urban soils.

3.2.2 Cd adsorption

The adsorption of Cd to the soil substrate is higher in the seam material compared to the original construction material. All retardation factors are higher for the seam material compared to the construction sand (Table 3). Compared to Pb, for Cd the improved sorption capacity is not a result of the deposition of OM, as there is no corellation between R and C_{org}, nor Cd_{tot} and C_{org}. So the deposition of other adsorbers,like Mn and Fe-oxides which have not been studied here, could be relevant. There is no difference in the adsorption behaviour of samples from Warsaw or Berlin of Cd.

Compared to natural sandy soils, the seam material shows a similar retardation of Pb but a low retardation of Cd. Kocher (2007) investigated sandy soils along federal highways in Germany for their HM retention while Adhikari and Singh (2003) investigated sandy soils from India and England (Table 4). The soils A1, A2, and A3 from Kocher (2007) had higher C_{org} (31, 50, and 50 g kg^{-1}) and slightly lower pH values (6.5,6.6, and 6.1)compared to seam materials but were comparable in terms of clay content (see Nehls et al., 2006). For a comparison, the retardation factors were computed for the same case like in Table 3. For Pb, the values are slightly, but not significantly higher. This is due to similar K_f, but low values for m (0.24, 0.18, and 0.08) indicating a highly non-linear adsorption favouring adsorption at low concentrations.

For Cd Kocher (2007) reports of similar m values, while the values for K_f are significantly higher in road side soils compared to seam materials. So, the Cd retardation in roadside soils is clearly higher compared to seam materials.

3.3 Simulated HM displacement

For the groundwater recharge rate of 120 mm a^{-1}, the simulated displacement times vary from 315 to 2350 a for Pb and from 37 to 253 a for Cd (Table 5). At the site B2, the measured dissolved equilibrium concentration of Pb in the soil is already higher than the concentration in the infiltrating surface water. For Cd, however all sites show higher soil water than rainwater concentrations. In these scenarios, every rainfall is a net HM displacement. Apart from these cases, the positive filter effects of urban depositions, which were already discussed by means of retardation factors, could be approved by the simulations for all cases but one. In the simulations, besides adsorption behaviour, also the soil hydraulic properties and the dry bulk densities were considered. The smaller dry bulk density of the seam material compared to the construction material results in a smaller number of adsorption sites per volume unit in the seam material although the number of adsorption sites per mass unit of the seam material is higher than in the original construction material. The displacement of Cd at the site B4 is the one example that shows this effect. If the scenarios *ia* and *iiia* for the site B4 are calculated with the original seam filling's dry bulk densities, the travel period through the seam material would be 105 a and therefore higher than that of the original seam filling. So except for the displacement of Cd at the site B4 we conclude that in general, the seam material has a positive impact on the retardation of Cd and Pb. Although the impact is detectable, it is not substantial and the formation of only 1 cm thick layer of seam material does not lead to longer travel periods. However, the potential of the urban dirt as a Pb filter is clearly to be seen if the scenarios *iiib* are compared to scenarios *ia*: even contaminated seam material is a much better filter than any clean construction sand. For Cd, the background contamination is that high, that both

Table 3. Heavy metal adsorption parameters of seam material from Berlin and Warsaw. K_f Freundlich's equilibrium constant, m Freundlich's exponent, c_{tot} total heavy metal concentrations in soil, R retardation factor, c_l dissolved concentraion, Θ soil water content, ρ_B dry bulk density.

Site	*Pb* K_f $mg^{1-m} L^m kg^{-1}$	*Pb* m	*Pb* r^2	*Pb* c_{tot} $mg\,kg^{-1}$	*Pb* R^a	*Cd* K_f $mg^{1-m} L^m kg^{-1}$	*Cd* m	*Cd* r^2	*Cd* c_{tot} $mg\,kg^{-1}$	*Cd* R^a
Berlin, 0 to 1 cm										
B1	2638[b]	1.00	0.87	68.5	19919	20.4	0.70	0.98	2.0	147
B2	2133[b]	1.00	0.71	91.0	15916	17.0	0.38	0.99	9.5	155
B4	1321	0.45	0.93	309.5	8685	19.4	0.62	0.99	n.d.	162
B5	977	0.44	0.96	290.2	6398	12.2	0.54	0.94	2.0	108
B6	1111	0.54	0.84	190.1	7901	12.2	0.21	0.93	6.1	82
B7	1376	0.93	0.96	222.0	10518	13.0	0.25	0.96	8.4	100
B8	1056	0.58	0.91	163.4	7653	16.5	0.29	0.98	6.9	121
B9	1416	0.62	0.86	203.5	10476	14.2	0.48	0.94	2.0	119
B10	2483	0.57	0.95	480.0	17914	15.2	0.28	0.98	6.1	110
Berlin, 1 to 5 cm										
B1a	499	0.92	0.96	38.3	3817	6.9	0.63	0.81	2.1	62
B2a	272[b]	1.00	0.99	49.6	2056	5.4	0.41	0.99	5.2	53
B4a	833	0.55	0.95	72.6	5961	5.7	0.40	0.69	4.0	43
B9a	738	0.62	0.93	135.6	5449	8.6	0.34	0.99	13.0	82
Warsaw, 0 to 1 cm										
W1	12558[b]	1.00	0.97	148.1	94817	20.3	0.30	0.98	2.9	145
W2	8052	0.89	0.97	180.9	61784	11.9	0.18	0.85	5.1	87
W3	4699	0.76	0.95	159.3	35982	12.1	0.15	0.76	5.5	77
W5	2738	0.91	0.87	99.7	20965	33.6	0.28	0.90	8.5	280
W8	2234	0.75	0.98	98.5	17088	8.4	0.10	0.89	5.2	42
W9	3078	0.88	0.89	270.7	23627	79.2	0.55	0.99	5.0	485

[a] ρ_B=1.5 g cm^{-3}, c_l=0.1 mg L^{-1}, Θ=0.3 m^3 m^{-3}
[b] isotherms were fitted with $0 \leq m \leq 1$

Table 4. Published adsorption data for soils comparable to seam material concerning organic matter and clay content.

soil	*Pb* K_f $dm^3\,kg^{-1}$	*Pb* m -	*Pb* R^a -	*Cd* K_f $dm^3\,kg^{-1}$	*Cd* m -	*Cd* R^a -
Kocher (2007)						
jAh,0 to 10 cm,A1,l m	6849	0.24	47118	120	0.50	949
jAh,0 to 25 cm,A2,l m	8495	0.18	50017	101	0.50	800
jAh,0 to 18 cm,A3,1 m	43720	0.08	143973	97	0.55	751
Adhikari and Singh (2003)						
Eng2, Norfolk	2239	0.73	15188	316	0.92	1752
Ind2, Ganges plains	102094	0.73	693895	1409	0.80	8973
Ind5, Desert sand	1135	0.42	9065	76	0.62	564

[a] ρ_B=1.5 g cm^{-3}, C_l=0.1 mg L^{-1}, Θ=0.3 m^3 m^{-3}

Table 5. Simulated heavy metal displacement through a 20 cm paved soil column at different sites in Berlin.

Scenario	*Pb*				*Cd*			
	B1	B2	B4	B9	B1	B2	B4	B9
	travel period[a] for 120 mm a^{-1}							
ia (uncontaminated sand)	610	315	1253	1072	37	92	100.8	176
ib (contaminated sand)	584	0	1159	1016	0	0	0	0
iia (uncontaminated sand with seam material)	612	320	1255	1075	39	93	101.4	179
iia (contaminated sand with seam material)	588	0	1158	1008	0	0	0	0
iiia (uncontaminated seam material)	2350	1901	1603	1578	90	185	83	253
iiib (contaminated seam material)	2350	1315	1341	1392	0	0	60	0

[a] indicate moment when 95% of applied concentration are detected at lower boundary

seam material and original construction sand act as a source rather than as a sink.

Because of the abundance of puddles at streets and sidewalks in urban areas, we simulated the infiltration of accumulated rainwater runoff from puddles. Realizing a higher infiltration rate of 0.48 instead of 0.12 cm d^{-1} influences the soil water content and therefore the pore water velocities. The average ratio between the traveltimes for 120 mm a^{-1} and 480 mm a^{-1} is 1/4. The calculated traveltimes range from 10 to 100 a for *Cd*. As the pavements at the investigated sites were constructed from the early 1900s on, a substantial mass of heavy metals may already have left the upper soil layers. The displacement risk for *Pb* even from puddles is rather low. However, the simulated infiltration from puddles shows the high importance of non-uniform infiltration in urban areas. It therefore underlines the need of knowledge on soil surface properties for realistic risk assessments, e.g. for more mobile substances such as glyphosate (Kempenaar et al., 2007).

4 Conclusions

Depositions of all kinds of urban dirt form the seam material, which has different properties than the original material. Compared to the original construction sand, the depositions lead to increased specific surface area and cation exchange capacity. Compared to natural OM this anthropogenic form of organic material has a rather small surface area and surface charge density which results in comparable low cation exchange capacity.

In terms of heavy metal mobilisation and retention the seam material can act as a filter and a source depending on the element. Thereby the source as well as the filter effect are low because of the typical thin layer of only 1 cm. The simulated break through times for one dimensional matric flow suggest, that there is no general risk of a groundwater contamination from traffic released *Cd* and *Pb*. However, the infiltration of rainwater from puddles can lead to fast displacement of *Cd*, which may leave the pavement system after only a decade. We conclude, that the seam material is a interesting model substrate to show the positive and negative impacts of deposited dust on ecological soil functions in urban areas.

Acknowledgements. We greatefully thank the DFG (WE 1125/18-1) and the Polish Academy of Sciences for funding. Furthermore, we thank especially H. Stoffregen for his help and discussions.

Edited by: P. Grathwohl

References

Adhikari, T. and Singh, M.: Sorption characteristics of lead and cadmium in some soils of India, Geoderma, 114, 81–92, 2003.

Aranovich, G.: The theory of polymolecular adsorption, Langmuir, 8, 736–739, 1992.

Boller, M.: Tracking heavy metals reveals sustainability deficits of urban drainage systems, Water Science and Technology, 35, 77–87, 1997.

Brunauer, S., Emmett, P. H., and Teller, E.: Adsorption of gases in multimolecular layers, Journal of the American Chemical Society, 60, 309–319, 1938.

Burghardt, W.: Soils in urban and industrial environments, Journal of Plant Nutrition and Soil Science, 157, 205–214, 1994.

Dannecker, W., Au, M., and Stechmann, H.: Substance Load in Rainwater Runoff from Different Streets in Hamburg, The Science of the Total Environment, 93, 385–392, 1990.

Dierkes, C. and Geiger, W. F.: Pollution retention capabilities of roadside soils, Water Science and Technology, 39, 201–208, 1999.

Griffin, R.A. and Jurinak, J.J.: Estimation of Activity-Coefficients from Electrical Conductivity of Natural Aquatic Systems and Soil Extracts, Soil Science, 116, 26-30, 1973.

Hajnos, M., Jozefaciuk, G., Sokolowska, Z., Greiffenhagen, A., and Wessolek, G.: Water storage, surface, and structural properties of sandy forest humus horizons, Journal of Plant Nutrition and Soil Science, 166, 625–634, 2003.

Harris, L.: Adsorption on a patchwise heterogeneous surface. I. Mathemantical analysis of the step function approximation of the local isotherm, Surface Science, 10, 129–145, 1968.

Heinzmann, B.: Improvement of the surface water quality in the Berlin region, Water Science and Technology, 38, 191–200, 1998.

Jaroniec, M. and Brauer, P.: Recent progress in determination of energetic heterogeneity of solids from adsorption data, Surface Science Reports, 6, 65–117, 1986.

Jozefaciuk, G. and Shin, J.: Water vapor adsorption on soils. II.Estimation of adsorption energy distributions using local BET and Aranovich isotherms, Korean Journal of Soil Science and Fertilizer, 29, 218–225, 1996.

Jozefaciuk, G., Toth, T. and Szendrei, G. (2006) Surface and micropore properties of saline soil profiles. Geoderma, 135, 1-15, 1996

Kempenaar, C., Lotz, L. A. P., van der Horst, C. L. M., Beltman, W. H. J., Leemnans, K. J. M., and Bannink, A. D.: Trade off between costs and environmental effects of weed control on pavements, Crop Protection, 26, 430–435, 2007.

Kocher, B.: Einträge und Verlagerung strassenverkehrsbedingter Schwermetalle in Sandböden an stark befahrenen Ausserortstrassen, in: Bodenökologie und Bodengenese 38, edited by Renger, M., Wessolek, G., Kaupenjohann, M. and Alaily, F. , Berlin : Fachgebiete Bodenkunde / Standortskunde und Bodenschutz, Institut für Ökologie, Technische Universität Berlin, 2007.

Krogh, L., Breuning-Madsen, H., and Greve, M. H.: Cation-exchange capacity pedotransfer functions for Danish soils, Acta Agriculturae Scandinavica Section B-Soil and Plant Science, 50, 1–12, 2000.

Mehlich, A.: Mehlich-3 soil test extractant: a modification of Mehlich-2 extractant, Communications in Soil Science and Plant Analysis, 15, 1409–1416, 1984.

Nehls, T., Jozefaciuk, G., Sokolowska, Z., Hajnos, M., and Wessolek, G.: Pore-system characteristics of pavement seam materials of urban sites, Journal of Plant Nutrition and Soil Science, 169, 16–24, 2006.

Novakov, T.: The role of soot and primary oxidants in atmospheric chemistry, The Science of the Total Environment, 36, 1–10, 1984.

OECD: OECD Guideline for the testing of chemicals No. 106: Adsorption - Desorption Using a Batch Equilibrium Method, 2000.

Parfitt, R., Giltrap, D., and Whitton, J.: Contribution of organic matter and clay minerals to the cation exchange capacity of soils, Communications in Soil Science and Plant Analysis, 26, 1343–1355, 1995.

Renger, M.: Berechnung der Austauschkapazität der organischen und anorganischen Anteile der Böden, Zeitschrift für Pflanzenernährung und Bodenkunde, 110, 10–26, 1965.

Simunek, J., Sejna, M., and vanGenuchten, M.: The HYDRUS-2D Software Package for Simulating the two-dimensional movement of water, heat, and multiple solutes in variably-saturated media, Tech. rep., U.S. Salinity Labaoratory, Riverside, CA 92507, 1999.

Sposito, G.: Derivation of the Freundlich Equation for Ion Exchange Reactions in Soils, Soil Science Society of America Journal, 44, 652–654, 1980.

Stumm, W. and Morgan, J.: Aquatic Chemistry, John Wiley and Sons, Inc., New York, 3 rd ed. edn., 1996.

Toth, T. and Jozefaciuk, G.: Physicochemical properties of a solonetzic toposequence, Geoderma, 106, 137–159, 2002.

Tryon, E.: Effect of charcoal on certain physical, chemical and biological properties of forest soils, Ecological Monographs, 18, 82–114, 1948.

Welp, G. and Brümmer, G. W.: Adsorption and solubility of ten metals in soil samples of different composition, Journal of Plant Nutrition and Soil Science, 162, 155–161, 1999.

Wessolek, G. and Facklam, M.: Standorteigenschaften und Wasserhaushalt von versiegelten Flächen, Journal of Plant Nutrition and Soil Science, 160, 41–46, 1997.

Wessolek, G. and Renger, M.: Bodenwasser- und Grundwasserhaushalt, in: Stadtökologie, edited by Sukopp, H. and Wittig, R., pp. 186–200, Gustav Fischer, Stuttgart, 1998.

Wilczynski, W., Renger, M., Jozefaciuk, G., Hajnos, M., and Sokolowska, Z.: Surface area and CEC as related to qualitative and quantitative changes of forest soil organic matter after liming, Journal of Plant Nutrition and Soil Science, 156, 235–238, 1993.